

Cite this: *Lab Chip*, 2011, **11**, 3593

www.rsc.org/loc

Automated high-throughput generation of droplets

Jan Guzowski,^a Piotr M. Korczyk,^{ab} Sławomir Jakiela^a and Piotr Garstecki^{*a}

Received 5th July 2011, Accepted 11th August 2011

DOI: 10.1039/c1lc20595a

We report a microfluidic technique for high-throughput generation of droplets of nanolitre volume in parallel channels with online control of the volumes, volume fraction and distribution of droplet volumes with the use of two external valves.

Industrial applications of droplet microfluidic systems in chemical synthesis¹ and formulation of particles^{2,3} and capsules⁴ require techniques for high-throughput generation of droplets. Microfluidic techniques provide attractive vistas to encapsulate biomaterials,⁵ prepare targeted drug delivery vehicles⁶ or control rate of release.⁷ An effort has thus been put to construct devices to produce droplets at high rates. The operation of different types of junctions (flow-focusing,⁸ T-junctions⁹ or concentric capillaries¹⁰) has been investigated in terms of their throughput and dependence of the volume of droplets on the flow rates. Such *passive* formation of droplets—*i.e.* generation of droplets with constant inflow of liquids—has drawbacks. For example the transition from dripping to jetting¹⁰ sets a limit on the frequency of generation. Also the volume of the droplets and their volume fraction both depend on the rates of flow and cannot be controlled independently. This dependence also makes the monodispersity of the emulsion vulnerable to fluctuations of the input rates of flow, the effect not desirable in applications.

Throughput of microfluidic chips can be increased in systems of parallel generators.¹¹ Integrated *passive* systems share similar limitations to those suffered by single junctions. The limitations in throughput or independent control of volume and volume fraction may in fact be even more severe in terms of, *e.g.*, the range of operational rates of flow due to the effects of coupling and cross-flow between junctions.

In recent years a number of groups reported *automated* systems with the delivery of the droplet phase *actively* controlled with a valve—either a pneumatic microvalve,^{12,13} a piezoelectric valve,¹⁴ or an active micro-reservoir.¹⁵ Churski *et al.*¹⁶ have shown that control of *both* of the immiscible phases provides a superior dynamic range of volumes of drops.

This system¹⁶ is perfectly suited for application to high-throughput parallel generation of droplets because it uses *external* valves. Here, we test the applicability of use of just two external—standard plunger type electromagnetic—valves (V165, Sirai, Italy) to control the

pressure driven flow of immiscible liquids through a parallel device and show that this simple system offers features that are required for industrial applications. These include: i) superior operational range of rates of flow, ii) superior range of volumes of droplets that can be formed, iii) full control over the distribution of droplet volumes, including the ability to form arbitrary sequences of droplet volumes, iv) superior range of volume fractions of the dispersed phase, controlled independently of throughput, and v) amenability to application of an online error-correction feedback that stabilizes the volumes of the droplets against fluctuations of the rate of flow from external reservoirs of liquids.

We prepared the microfluidic device by micromilling three polycarbonate sheets, put them in oxygen plasma for 2 min and then bonded them in a hydraulic press (1 MPa, 120 °C). The chip comprised two sets of 16 channels of 200 μm width, each supplied with a different liquid. The channels merged in 16 T-junctions (Fig. 1). The inlet and outlet channels of the junctions were relatively long (3 cm and 1.5 cm, respectively) to minimize the effects of hydrodynamic coupling between the junctions and to equate the rates of flow through them.

We used silicone oil as the continuous phase and fluorinated oil (FC40) as the droplet phase, both supplied from external pressurized containers through thin (200 μm) and long (0.5 m) steel capillaries that increased the hydrodynamic resistance of the whole system and minimized the relative fluctuations of the resistance due to the presence of droplets in the channels.¹⁷

We investigated two operational modes of the device: (i) *passive*, in which the liquids were supplied under constant rates of flow, and (ii) *active*, in which the flows were controlled by the external valves. In the *passive* mode we adjusted the volume of the droplets V and their volume fraction ϕ by changing the applied flow rates q_c and q_d of the continuous and the droplet phases, respectively (see Fig. 2a and 2b). In the *active* mode we adjusted V and ϕ independently by setting four

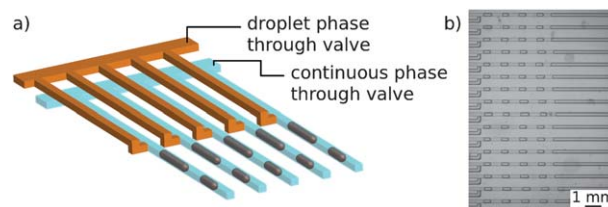


Fig. 1 (a) Schematic representation of the microfluidic device for automated production of droplets in multiple channels. (b) A micrograph of the outlet channels with droplets of various lengths.

^aInstitute of Physical Chemistry, Polish Academy of Sciences, Warsaw, Poland. E-mail: garst@ichf.edu.pl

^bInstitute of Fundamental Technological Research, Polish Academy of Sciences, Warsaw, Poland

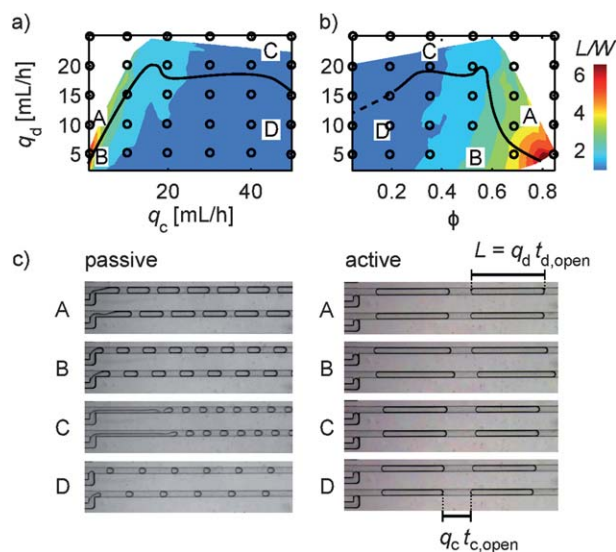


Fig. 2 Color-coded normalized length of droplets (without valves) as a function of the flow rates q_c and q_d (a) or the volume fraction $\phi = q_d/(q_d + q_c)$ and q_c (b). Solid lines indicate the dripping-jetting transition (see, e. g., (c)-passive). The dashed line is an extrapolation (for $q_c > 50 \text{ mL h}^{-1}$). Open symbols mark the spots in which we tested formation of drops (length $L = q_d t_{d, \text{open}}$) in the active mode. The volume fraction $\phi = q_d t_{d, \text{open}}/(q_d t_{d, \text{open}} + q_c t_{c, \text{open}})$ is independent of q_c and q_d , in contrast to the case of the passive mode (c). Note that in the active mode the droplets are produced synchronously in all channels (here only 2 of all 16 channels are displayed).

parameters: q_d , q_c and the opening times of the valves $t_{d, \text{open}}$, $t_{c, \text{open}}$.¹⁶ During the time $t_{d, \text{open}}$ the droplet phase flowed through the junction, while the external phase was turned off. Next, the droplet phase was turned off and the continuous phase was turned on for the time $t_{c, \text{open}}$. Accordingly the droplets of volume $q_d t_{d, \text{open}}$ were formed and separated by the continuous phase of volume $q_c t_{c, \text{open}}$ (Fig. 2(c)).

In the *passive* mode the droplets were only formed for $q_d < q_{d, \text{crit}}$, where $q_{d, \text{crit}} = q_{d, \text{crit}}(q_c)$ (see the color-coded map in Fig. 2a), whereas for $q_d > q_{d, \text{crit}}$ the droplets were not formed at all and we observed a transition to a laminar co-flow of both liquids. More precisely, upon increasing q_d we could distinguish the regimes of squeezing, dripping and jetting similarly to the case of a single T-junction.¹⁸ Accordingly, the throughput of the device was limited by the jetting transition (see Fig. 2a). In contrast, in the *active* mode the production of the droplets within the available range of rates of flow (i.e., not exceeding 50 mL h^{-1}) was not limited by any critical flow rate (Fig. 2a and 2c).

In the *passive* mode the volume fraction ϕ can be calculated as $\phi = q_d/(q_d + q_c)$. However, due to the jetting transition certain values of the volume fraction could not be obtained at all (see Fig. 2b). This limitation was absent in the *active* mode. With the valves turned on we have $\phi = q_d t_{d, \text{open}}/(q_d t_{d, \text{open}} + q_c t_{c, \text{open}})$, which means that even for a given q_d and q_c we could always tune ϕ by adjusting the opening times $t_{d, \text{open}}$ and $t_{c, \text{open}}$ of the valves. As a consequence the range of the available volume fractions was much larger (Fig. 2b). The upper limit on the volume fraction for a given droplet volume V was set in this case by the time $\Delta t \approx 10 \text{ ms}$ needed to open or close the valve. Accordingly, the minimal volume of the continuous phase was $2q_c \Delta t$ and the maximum volume fraction $\phi_{\text{max}}(V) = V/(V + 2q_c \Delta t)$.

The use of the valves also improved the control over the volume V of the droplets (or equivalently their length L in the channels, see

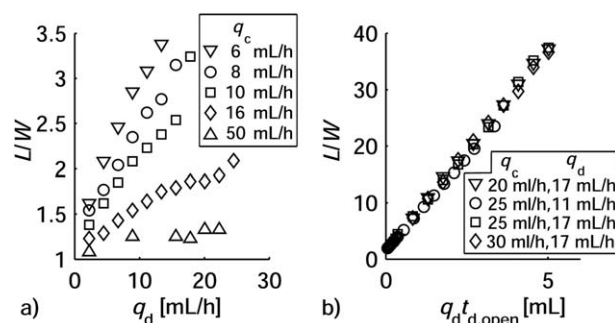


Fig. 3 (a) Length of droplets vs. q_d for various values of q_c . Data terminate at the length corresponding to the transition to jetting, above which the droplets are not formed at all. (b) In the active mode there is no limiting value on the maximal length.

Fig. 3a and 3b). In the *passive* mode (Fig. 3a) V is a function not only of the flow rates but also of the geometry and size of the junction as well as of the material parameters such as viscosities and surface tensions of the liquids. The actual formula for V depends on the mechanism of formation of the droplets (squeezing,⁹ dripping¹⁹ or jetting¹⁰) and usually cannot be given analytically. In contrast, in the *active* mode a simple formula $V = q_d t_{d, \text{open}}$ perfectly reproduces our experimental data (Fig. 3b).

Automation of the production of droplets has an additional qualitative advantage in that the volume of the droplets can be controlled on-line independently of the applied rates of flow. We used a camera operated on-line by an image processing software that triggered the valves depending on the detected image. For example, the droplet phase was triggered off when a droplet reached the desired length, allowing production of monodisperse droplets in all channels regardless of the changes in the rates of external supply of the liquids (see Fig. 4). A small but noticeable linear dependence on q_d in Fig. 4 was an artefact of a finite opening time Δt of the valves ($\approx 10 \text{ ms}$) and can be eliminated with more sophisticated feedback algorithms that take into account the momentary rate of growth of the droplet or with valves that provide a shorter response time (e.g. piezoelectric actuators).

To demonstrate control over the distribution of volumes of droplets we encoded a picture of Marilyn Monroe into a sequence of droplets (Fig. 5). We resolved 100 different lengths of droplets, providing a resolution of $100 \text{ px} \times 100 \text{ px}$ of the image. The x_i and y_i coordinates of pixel i were associated with lengths of i -th pair of

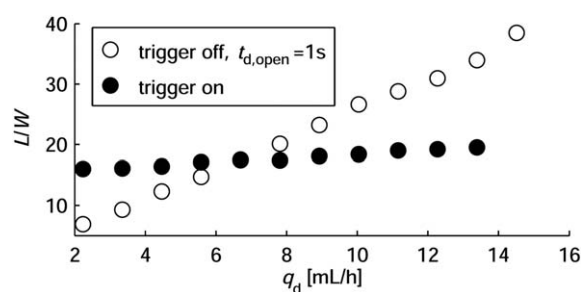


Fig. 4 In the active mode and for fixed $t_{d, \text{open}}$ the length of the droplets depends linearly on the flow rate q_d (open symbols). Independence of the flow rate is achieved by triggering the flow of the droplet phase off each time the droplets reach the desired length (solid symbols).

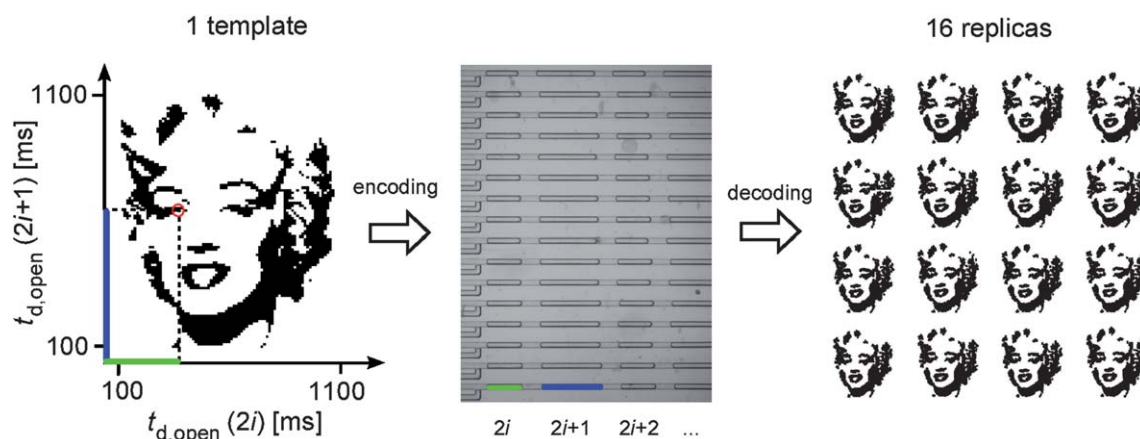


Fig. 5 We encoded a picture of Marilyn Monroe in resolution $100 \text{ px} \times 100 \text{ px}$ (left panel) in the sequence of droplets of 100 different volumes corresponding to the opening times $t_{d, \text{open}}$ from 100 to 1100 ms with a step of 10 ms in 16 parallel channels (middle panel). We numbered the pixels in the original picture from left to right and from top to bottom so that $i = 0$ was associated with the left-most pixel in the top row. We decoded the positions of the pixels and reproduced the picture in 16 copies (right panel) by measuring the lengths of the droplets from the micrographs by means of the electronic image processing.

droplets, *i.e.*, $(x_i, y_i) = (L_{2i}, L_{2i+1})$. We programmed a sequence of times $t_{d, \text{open}}$, executed the protocol and recorded the lengths of droplets produced in each of 16 channels. Next we analyzed the lengths of the drops with an image processing software (MATLAB) to produce the 16 images shown in Fig. 5 (right panel) that faithfully reproduced the original picture (one can notice small defects which occurred due to contamination of the field of view of the camera, *e.g.*, by dust).

In conclusion, we have developed a microfluidic device for high-throughput, on-demand formulation of droplets in which the liquids are supplied *via* two external valves and the flow is multiplexed into 16 parallel channels without loss of control over generation of the droplets. Automated formation of droplets has important advantages over *passive* methods in that i) the regime of the available rates of flow is much larger (Fig. 2a), ii) there is no upper limit on the volume of the droplets (Fig. 3) and no limit at all on their volume fraction (Fig. 2b), iii) the volume and the volume fraction can be controlled independently by changing the opening times of the valves (Fig. 2), iv) the system provides superior monodispersity of the droplets robust against fluctuations in the rates of flow (Fig. 4), v) it is possible to formulate arbitrary sequences of volumes of droplets (Fig. 5). Our device provides unlimited volumes and superior volume fraction with on-line control. It can also be used to produce emulsions composed of droplets of various volumes spanning orders of magnitude (Fig. 5). Importantly—as any effects associated with a finite dead volume or finite relaxation time of the valve are distributed equally between the parallel junctions—the method should be directly applicable to systems of smaller channels and to systems comprising much larger number of channels operated with just two external valves.

Acknowledgements

Project operated within the Foundation for Polish Science Team Programme co-financed by the EU European Regional Development

Fund. J.G. acknowledges financial support from the Polish Ministry of Science under the grant Iuventus Plus.

References

- 1 H. Song and R. F. Ismagilov, *J. Am. Chem. Soc.*, 2003, **125**, 14613–14619.
- 2 Z. Nie, W. Li, M. Seo, S. Xu and E. Kumacheva, *J. Am. Chem. Soc.*, 2006, **128**, 9408–9412.
- 3 D. Lee and D. A. Weitz, *Small*, 2009, **5**, 1932–1935.
- 4 A. R. Abate, C. Chen, J. J. Agresti and D. A. Weitz, *Lab Chip*, 2009, **9**, 2628.
- 5 E. Um, D. S. Lee, H. B. Pyo and J. K. Park, *Microfluid. Nanofluid.*, 2008, **5**, 541.
- 6 S. R. Sirsi and M. A. Borden, *Bubble Sci., Eng. Technol.*, 2009, **1**, 3.
- 7 Q. Xu, M. Hashimoto, T. T. Dang, T. Hoare, D. S. Kohane, G. M. Whitesides, R. Langer and D. G. Anderson, *Small*, 2009, **5**, 1575.
- 8 P. Garstecki, H. A. Stone and G. M. Whitesides, *Phys. Rev. Lett.*, 2005, **94**, 164501.
- 9 P. Garstecki, M. J. Fuerstman, H. A. Stone and G. M. Whitesides, *Lab Chip*, 2006, **6**, 437.
- 10 P. Guillot, A. Colin, A. S. Utada and A. Ajdari, *Phys. Rev. Lett.*, 2007, **99**, 104502.
- 11 T. Nisisako and T. Torii, *Lab Chip*, 2008, **8**, 287–293.
- 12 Y. Zheng, W. Dai and H. Wu, *Lab Chip*, 2009, **9**, 469.
- 13 K. Churski, J. Michalski and P. Garstecki, *Lab Chip*, 2010, **10**, 512.
- 14 A. Bransky, N. Korin, M. Khoury and S. Levenberg, *Lab Chip*, 2009, **9**, 516.
- 15 J. Xu and D. Attinger, *J. Micromech. Microeng.*, 2008, **18**, 065020.
- 16 K. Churski, P. M. Korczyk and P. Garstecki, *Lab Chip*, 2010, **10**, 816–818.
- 17 P. M. Korczyk, O. Cybulski, S. Makulska and P. Garstecki, *Lab Chip*, 2011, **11**, 173–175.
- 18 P. Guillot and A. Colin, *Phys. Rev. E: Stat., Nonlinear, Soft Matter Phys.*, 2005, **72**, 066301.
- 19 M. De Menech, P. Garstecki, F. Jousse and H. A. Stone, *J. Fluid Mech.*, 2008, **595**, 141–161.